Validation of the 3D stochastic turbulence reconstruction method with the Gaussian filter

V. Korchagin [1], **B. Vanelderen** [1], **W. De Roeck** [1], **W. Desmet** [1,2]
[1] KU Leuven, Department of Mechanical Engineering,
Celestijnenlaan 300, B-3001, Leuven, Belgium
e-mail: **vyacheslav.korchagin@kuleuven.be**

[2] member of Flanders Make

Abstract
This paper describes a synthetic turbulence reconstruction method based on filtering of the white noise field and convection of the particles by means of the Random Particle Mesh method (RPM) in three dimensions. For that purpose a Gaussian filter is derived from the Gaussian energy spectrum. The method is applied to simple threedimensional geometry. The parametric study is performed in order to analyse the sensitivity of the method to several computational parameters. The retrieved statistics of the flow is then compared to the analytical solution. The results of the research suggest an optimal choice of these parameters to obtain the accurate numerical solution. The parallel performance of the hybrid MPI-OpenMP implementation of the method is shown.

1 Introduction

Prediction of the behaviour of the aero-acoustic interactions between sound and flow remains a challenging task for both researchers and engineers. A trade-off between the computational performance and the precision of the solution has to be made. Powerful computational machines solve more complicated problems and produce more accurate results. Most of the academic studies are still carried out in two dimensions, whereas real problems including turbulence are always in three dimensions. To apply methods originally developed in 2D to 3D problems, efficient and accurate algorithms should be implemented and validated.
Both sound wave propagation in flow as well as sound source generation are an unsteady phenomena. A straightforward way to study this is to use an unsteady wave propagation solver coupled with an unsteady CFD solver for noise generation, e.g. Large Eddy Simulation. This coupling will produce accurate results, but due to the high computational requirements, these methods are mostly used in academics.
Stochastic methods for the turbulent flow reconstruction use steady CFD solutions, e.g., RANS, to generate synthetic unsteady turbulence.
Stochastic methods based on Fourier modes were introduced by Kraichman [1] and later augmented by Karweit [2]. Bechara [3] and Baily [4] developed a Stochastic Noise Generation and Radiation (SNGR) method that generated a non-stationary velocity field and used mean flow. The SNGR method was coupled with linearised Euler equation solver to simulate noise radiation and generation for free and wall-bounded flows. Blom et al. [5] and Billson et. al [6] applied this method to external wall-bounded flow and free jet, respectively.
Filter based methods were originally described by Careta et. al [7]. To synthesize the turbulence flow, white-noise field had to be filtered [8]. Ewert et. al extended the method by inserting particles that propagate along streamlines [9] introducing Random Particle Mesh (RPM) method and later improved its computational performance in fast RPM (fRPM). When the latter team focused their efforts on Gaussian filters, Dieste and

Gabard [10] carried out their research also with von Kármán and Liepmann filters. Vanelderen [11] combined approaches of Ewert and Dieste to validate the RPM method in two dimensions for free jet flow and a slit configuration.
The work presented here extends the research of Vanelderen to three dimensional cases. The study is limited to the filter derived from the 3D Gaussian energy spectrum and shows the sensitivity of the method to computational parameters, such as simulation time, sampling rate and particle density. The method was parallelized using a hybrid MPI-OpenMP approach of which the performance is described here as well.

2 Theory

2.1 Description of the filtering function in 3D

For the incompressible flow, the velocity vector, $\mathbf{u}'$ can be derived from the stream function ψ' as:

$$\mathbf{u}' = \nabla \times \psi', \tag{1}$$

in vector notation:

$$\left(U_1', U_2', U_3'\right)^T = \left[\left(\frac{\partial \psi_3}{\partial x_2} - \frac{\partial \psi_2}{\partial x_3}\right), \left(\frac{\partial \psi_1}{\partial x_3} - \frac{\partial \psi_3}{\partial x_1}\right), \left(\frac{\partial \psi_2}{\partial x_1} - \frac{\partial \psi_1}{\partial x_2}\right)\right]^T, \tag{2}$$

According to Ewert,et. al[9] streamfunction can be obtained by filtering white-noise field

$$\psi'(\mathbf{x}, t) = \int_{\mathbb{R}^3} G(|\mathbf{x} - \mathbf{x}'|)\mathcal{U}(\mathbf{x}', t)d\mathbf{x}' \tag{3}$$

where $\mathcal{U}$ is white noise field with zero mean, $\mathbf{x}'$ - particle position coordinates, and $\mathbf{x}$ - evaluation point coordinates.

$$\overline{\mathcal{U}(\mathbf{x})} = 0. \tag{4}$$

The two-point spatial correlation of the velocity vector component,$R_{ij}(r)$, is given by

$$R_{ij}(r) =< U_i(x), U_j(x + r) >, \tag{5}$$

. The velocity correlation, $R(r)$, will be written futher as a trace of the two-point spatial correlation of the velocity vector

$$R(r) = \frac{1}{2}R_{ii(r)}. \tag{6}$$

And the two-point spatial correlation of the stream function is given by

$$C_{ij}(r) =< \psi_i(x), \psi_j(x + r) > . \tag{7}$$

The streamfunction correlation and the velocity correlation are related[12], we can derive a filter expression from the energy spectrum formulation. Derivation of the filter function from the correlation functions is demonstrated by Dieste and Gabard [10] but is out of scope of current research.

The correlation of the the stream function in terms of the filter function is given as [10]

$$C(r) = (G * G)(r), \tag{8}$$

or in wavenumber domain

$$C(k) = \hat{G}(\kappa)^2, \tag{9}$$

where $*$ is a spatial 3D convolution operator.

The Fourier-Bessel transform, assuming isotropic turbulence, is defined as

$$F(r) = \frac{1}{2\pi^2} \int_0^\infty \hat{F}(\kappa)\kappa^2 j_0(\kappa r) d\kappa. \tag{10}$$

where $j_0(\kappa r) = \frac{sin(\kappa r)}{\kappa r}$ is the 0-th order spherical Bessel function of the first kind.

To express the stream function correlation in physical coordinates the Fourier-Bessel transform (10) is applied to the streamfunction correlation resulting in

$$C(r) = \frac{1}{2\pi^2} \int_0^\infty \hat{G}(\kappa)^2\kappa^2 j_0(\kappa r) d\kappa. \tag{11}$$

Two-point correlation of the velocity field (Eq. (5)) can be expressed in terms of lateral and transverse correlation functions $f(r)$ and $g(r)$, respectively,

$$R_{ij}(r) = g(r)\delta_{ij} + [f(r) - g(r)] \frac{r_i r_j}{r^2}, \tag{12}$$

These correlation functions can be derived from the streamfunction correlation as follows

$$f(r) = -\frac{2}{r}\frac{dC(r)}{dr}, \tag{13}$$

$$g(r) = -\frac{d^2C(r)}{dr^2} - \frac{1}{r}\frac{dC(r)}{dr}. \tag{14}$$

The velocity correlation (6) can be expressed in terms of streamfunction correlation

$$R(r) = -\frac{d^2C(r)}{dr^2} - \frac{2}{r}\frac{dC(r)}{dr}. \tag{15}$$

This expression can be written now in terms of the filter spectrum by use of Eq. (11)

$$R(r) = \frac{1}{2\pi^2} \int_0^\infty \kappa^2\hat{G}(\kappa)^2\kappa^2 j_0(\kappa r) d\kappa. \tag{16}$$

From Eq. (16) and Eq. (10) one can conclude that

$$\hat{R}(\kappa) = \kappa^2\hat{G}(\kappa)^2. \tag{17}$$

The following step, to derive the filter function, is to relate the energy spectrum to the velocity spectrum. This is done by integrating the velocity spectrum over the surface of a sphere $S(\kappa)$ with radius κ and center in the origin:

$$E(\kappa) = \oint \frac{1}{2}\phi_{ii}(\boldsymbol{\kappa}) dS(\kappa), \tag{18}$$

where $\kappa = |\boldsymbol{\kappa}|$ is the magnitude of all wavenumbers $\boldsymbol{\kappa}$. Knowing that $\oint dS(\kappa) = 4\pi\kappa^2$

$$E(\kappa) = 2\pi\kappa^2\phi_{ii}(\boldsymbol{\kappa}). \tag{19}$$

The velocity spectrum is related to its correlation via

$$\phi_{ij}(\kappa) = \frac{1}{8\pi^2} \int_{\mathbb{R}^3} R_{ij}(r) e^{-i\boldsymbol{\kappa}\boldsymbol{r}} d\boldsymbol{r}. \tag{20}$$

Then the trace of the velocity spectrum in wavenumber space is,

$$\hat{R}(\kappa) = \frac{1}{2}\phi_{ii}(\kappa). \tag{21}$$

From Eq. (17), Eq. (21) and Eq. (19) follows the dependency of the energy spectrum on the filter function:

$$E(\kappa) = 4\pi\kappa^4\hat{G}(\kappa)^2. \tag{22}$$

And in the wave number domain the filter can be expressed in terms of energy spectrum

$$G(\kappa) = \frac{1}{2\kappa^2}\sqrt{\frac{E(\kappa)}{\pi}}. \tag{23}$$

The Fourier-Bessel transform finally yields the filter in physical domain

$$G(r) = \frac{1}{4\pi^{\frac{3}{2}}}\int_0^\infty \sqrt{E(\kappa)}j_0(\kappa r)d\kappa, \tag{24}$$

where $E(\kappa)$ is an energy spectrum, $r = \sqrt{x_1^2 + x_2^2 + x_3^2}$ is a distance between the particle and a computational node, i.e. $x_i = \mathbf{x}_i - \mathbf{x}_i'$.

3 Parametric study of the RPM method with the Gaussian filter

In this chapter we perform several parametric studies of the computational model to identify optimal values for efficient and accurate solutions assuming Gaussian energy spectrum in 3D given by reads [13]

$$E_g(\kappa) = \frac{8}{3\pi^3}K\lambda^5\kappa^4 e^{-\frac{\lambda^2\kappa^2}{\pi}}. \tag{25}$$

Note, that for 2D flow the filter reads

$$E_g(\kappa) = \frac{2}{\pi^2}K\lambda^4\kappa^3 e^{-\frac{\lambda^2\kappa^2}{\pi}}. \tag{26}$$

The respective filter in physical domain can be obtained using Eq. (24)

$$G_g(r) = \frac{1}{2\pi^2}\sqrt{\frac{K}{3\lambda}}e^{-\frac{\pi r^2}{2\lambda^2}} \tag{27}$$

or in Cartesian coordinates

$$G_g(x_1, x_2, x_3) = \frac{1}{2\pi^2}\sqrt{\frac{K}{3\lambda}}e^{-\frac{\pi\left(x_1^2+x_2^2+x_3^2\right)}{2\lambda^2}} \tag{28}$$

Assuming the Eulerian frame of reference, Eq. (3) for a computational node i and surrounding control volume j-th component of the stream function can be rewritten as the summation of the filtered 3-dimensional strength vector $\mathcal{U} = (\mathcal{U}_1, \mathcal{U}_2, \mathcal{U}_3)^T$ of all N particles in this volume

$$\psi_j^i = \sum_{n=1}^{N} G(|\mathbf{x}^i - \mathbf{x}_n'|)\mathcal{U}_j(\mathbf{x}_n', t) \tag{29}$$

and inserting the latter expression into Eq. (2) gives the velocity vector components

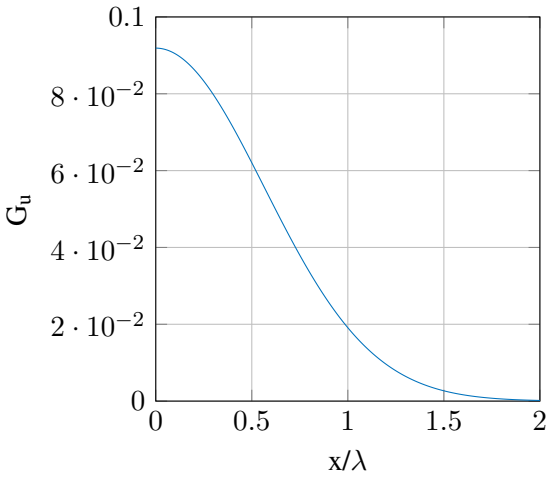

Figure 1: Derivative of the Gaussian filter with respect to integral lengthscale

[xMin; xMax]	nx	[yMin; yMax]	ny	[zMin; zMax]	nz	dx
[0; 1]	65	[0; 0.5]	33	[0; 0.5]	33	$\lambda/4$

Table 1: Domain for velocity correlation study

$$U_1^i = \sum_{n=1}^{N} \left(\frac{\partial \left[G(|\mathbf{x}^i - \mathbf{x}'_n|) \mathcal{U}_3(\mathbf{x}'_n, t) \right]}{\partial x_2} - \frac{\partial \left[G(|\mathbf{x}^i - \mathbf{x}'_n|) \mathcal{U}_2(\mathbf{x}'_n, t) \right]}{\partial x_3} \right), \tag{30}$$

$$U_2^i = \sum_{n=1}^{N} \left(\frac{\partial \left[G(|\mathbf{x}^i - \mathbf{x}'_n|) \mathcal{U}_1(\mathbf{x}'_n, t) \right]}{\partial x_3} - \frac{\partial \left[G(|\mathbf{x}^i - \mathbf{x}'_n|) \mathcal{U}_3(\mathbf{x}'_n, t) \right]}{\partial x_1} \right), \tag{31}$$

$$U_3^i = \sum_{n=1}^{N} \left(\frac{\partial \left[G(|\mathbf{x}^i - \mathbf{x}'_n|) \mathcal{U}_2(\mathbf{x}'_n, t) \right]}{\partial x_1} - \frac{\partial \left[G(|\mathbf{x}^i - \mathbf{x}'_n|) \mathcal{U}_1(\mathbf{x}'_n, t) \right]}{\partial x_2} \right) \tag{32}$$

where $\mathcal{U}_i$ are the independent spatial-temporal fields with zero mean, unity variance and cross correlation equal to zero, i.e. $< \mathcal{U}_i, \mathcal{U}_j >= 0$. The filter function, as well as its derivatives, are symmetric in all directions. In Fig. 1 the plot of a derivative of a filter function, $G_u = \partial G(x_1, x_2, x_3)/\partial x_1$ is depicted with respect to the turbulent length scale. The filter function decays exponentially and its value tends to zero at the distance of 2λ. Hence, we can limit our control volume by a sphere with radius $r = 2\lambda$, or to increase computational performance, by a cube with a side $a = 4\lambda$.

Parametric studies The parametric studies are performed on the domain described in Table 1.

The turbulence is considered to be frozen, i.e. no temporal change in the the particle strength is applied in the Lagrangian frame of reference

$$\frac{D_0}{Dt} \mathcal{U} = 0, \tag{33}$$

where $\frac{D_0}{Dt}$ is the material derivative. In addition, mean flow and simulation parameters were chosen, as listed in Table 2.

Parameter	Value	Distribution
K	1	uniform
λ	0.0625	
U	(1,0,0)	
Δt	0.01	

Table 2: Simulation and mean flow parameters.

a) **Variable simulation time.** To perform this study we run the simulation until it reaches 20k timesteps. Keeping a particle-per-volume (we consider a "volume" being a cube with a side equal to Δx) ratio equal to one, we compute velocity correlations R_{11} and R_{22} from the timestep 0 and till i) 5000, ii) 10 000, iii) 15 000, iv) 20 000. Figure 2a and Figure 2b show velocity correlations. Figure 2a demonstrates that the correlation R_{11}, or streamwise correlation, does not change significantly with increasing number of timesteps. Whereas the correlation R_{22}, or lateral correlation, in Figure 2b improves with longer simulation time.

b) **Variable sampling rate.** Fixing the simulation time at 20 000 timesteps, we now vary the sampling rate. The velocity data is collected every i) 10; ii) 5; iii) 2; iv) 1 timesteps. The resulting correlations are shown in a Figure 3. For correlation R_{11} there is no significant difference observed, whereas the correlation R_{22} shows small deviation from analytical solution when taken only 2 000 samples.

c) **Variable particles-per-volume ratio.** The last set of numerical experiments were carried out to determine the impact of the particles-per-volume (ppv) ratio on the correlation functions. The results of a simulation were post-processed after 10k timesteps for i) 1 ppv; ii) 2 ppv; and iii) 4 ppv. The closest fit to analytical solution is achieved by using 4 ppv as shown in Figure 4. When using 2 ppv the correlation curves start showing oscillating behaviour, and with only 1 ppv the curves slightly deviate from the analytical solution preserving the oscillating trend.

From these numerical experiments we can conclude that we need to run the simulation long enough to achieve desired statistics of the flow. As observed in the study "a)", 10 000 timesteps of the simulation is sufficient for the correlation curve to approach the analytical solution. Also, it is not necessary to take the samples every timestep as shown in the study b). Sometimes too small timesteps result in a slow propagation of information and by taking samples too often we end up with almost similar data sets. Another way to improve the quality of the simulation is to insert more particles. As shown in the study c), 2 ppv ratio produces much accurate solution compared to 1 ppv. However, having 4 ppv leads to double computational load, compared to 2 ppv, while improving the statistics insignificantly.

Parallel performance All experiments were carried out by a parallel hybrid MPI-OpenMP in-house RPM solver. The domain was split into n subdomains equal to the number of processor sockets, such that 1 MPI proccess is assigned per socket and, hence, per subdomain. Within a subdomain the main computational loop is parallelized with the OpenMP with the number of threads equal to the number of cpu's per socket.
The performance of the hybrid MPI-OpenMP parallelization is measured on the IvyBridge nodes of the VSC [1]. Each IvyBridge node consists of 2 sockets with 10 cores each. Picture 5 shows a near-linear speed up for the strong scaling performed in the same domain as parametric studies earlier.

[1] Vlaams Supercomputer Centrum - Flemish Supercomputer Centre cluster. For the simulations the thin node section was used, which consists of 208 nodes with two 10-core "Ivy Bridge" Xeon E5-2680v2 CPUs (2.8 GHz, 25 MB level 3 cache). 176 of those nodes have 64 GB RAM while 32 are equiped with 128 GB RAM. The nodes are linked to a QDR Infiniband network. [14]

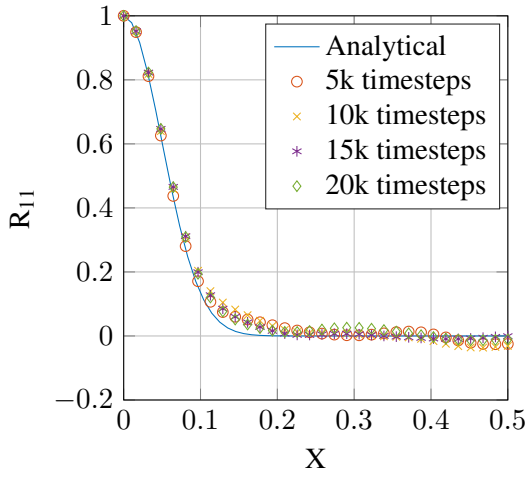

(a) R_{11} Velocity correlation

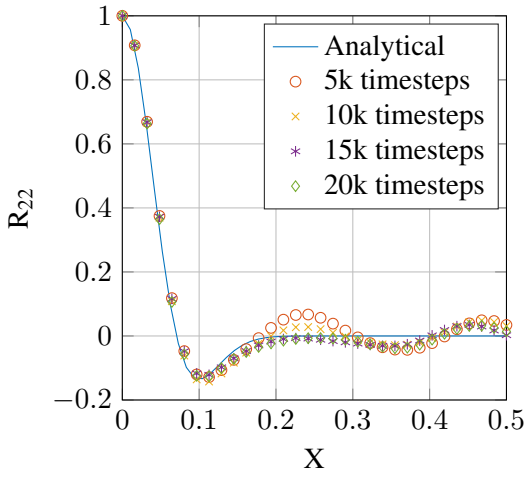

(b) R_{22} Velocity correlation

Figure 2: Correlations for variable simulation time

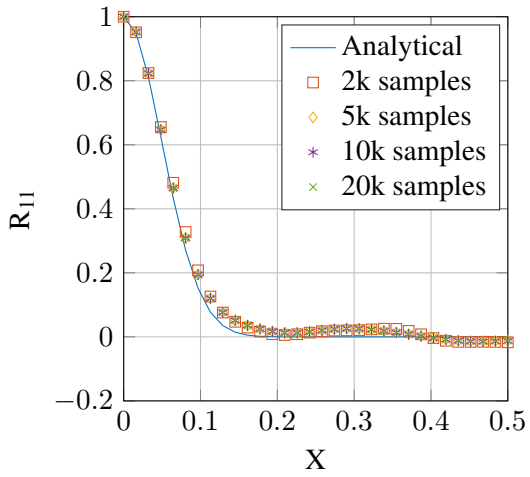

(a) R_{11} Velocity correlation

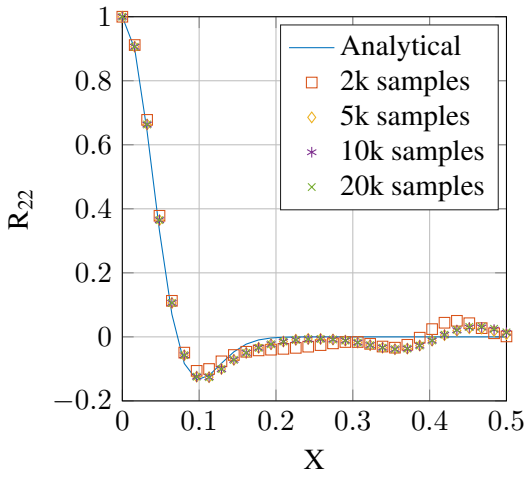

(b) R_{22} Velocity correlation

Figure 3: Correlations for variable sampling rate. Simulation time fixed to 20k timesteps

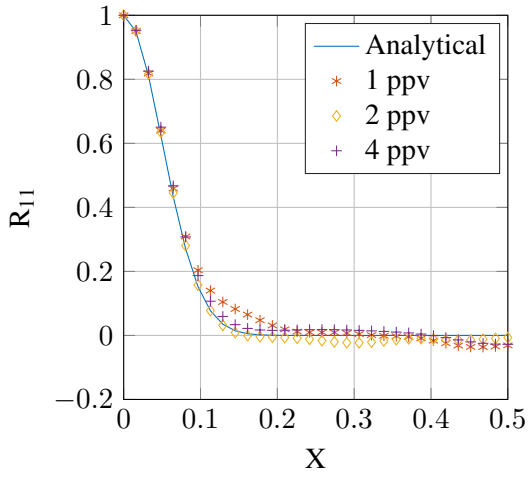

(a) R_{11} Velocity correlation

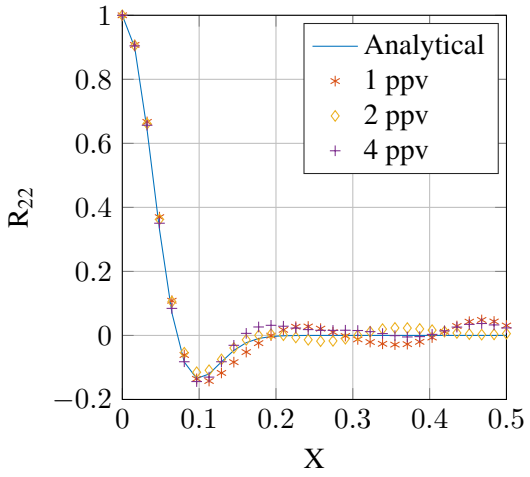

(b) R_{22} Velocity correlation

Figure 4: Correlations for variable ppv. Simulation time fixed to 20k timesteps

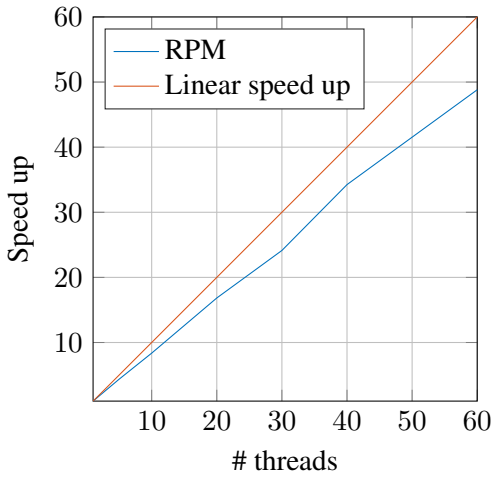

Figure 5: Parallel performance of the hybrid MPI-OpenMP RPM solver

4 Conclusions and future work

The aim of this paper is the validation of the flow statistics, generated by the RPM method, in three dimensions. The Gaussian filter was derived from the Gaussian energy spectrum. Secondly, this filter was applied to the white-noise field to reconstruct unsteady synthetic velocity field of a frozen turbulent flow. A control volume was defined of a size $2\lambda \times 2\lambda \times 2\lambda$ within which particles contribute significantly to the solution. Other parameters that affect the simulation accuracy were investigated, namely, simulation time, sampling rate and particle density. It was concluded that after certain simulation time the improvement of the solution is barely observed, thus, running the simulation for shorter time could still produce a correct statistical description of the flow. The sampling frequency should be chosen in such a way that the data in the consequent samples would differ and not stay almost unchanged. A sensitivity study of the particle density showed that a too sparse distribution of particles does not produce accurate correlation curves. It was also concluded that having too dense particle distribution only increases computational load without moving the correlation curve significantly closer to the analytical solution.
More studies will be performed to analyse the behaviour of the 3D RPM solver: non-frozen turbulence should be evaluated to ensure a correct time-decorrelation model; filters other than Gaussian are also to be investigated; as well as the analytical implementation of the filter will be substituted with polynomial approximation to speed-up the computations. Further, this solver will be coupled with the parallel Discontinuous Galerkin solver to propagate the sound generated by the pseudo-random RPM velocity field. The resulting tool will allow us to study noise generation and propagation phenomena in a three dimensional aero-acoustic domains.

Acknowledgements

The Fund for Scientific Research – Flanders (FWO) is gratefully acknowledged for its support, as well as The Research Fund KU Leuven. Also this research was partially supported by Flanders Make, the strategic research centre for the manufacturing industry. The computational resources and services used in this work were provided by the VSC (Flemish Supercomputer Center), funded by the Research Foundation - Flanders (FWO) and the Flemish Government – department EWI.

References

[1] R. Kraichnan, *Decay of Isotropic Turbulence in the Direct-Interaction Approximation*, Physics of Fluids, Vol. 7, No. 7, (1964), pp. 1030.

[2] M. Karweit, P. Blanc-Benon, D. Juvé, G. Comte-Bellot, *Simulation of the propagation of an acoustic wave through a turbulent velocity field: A study of phase variance*, The Journal of the Acoustical Society of America, Vol. 89, No. 1, (1991), pp. 52–62.

[3] W. Bechara, C. Bailly, P. Lafon, S. Candel, *Stochastic approach to noise modeling for free turbulent flows*, AIAA Journal, Vol. 32, No. 3, (1994), pp. 455–463.

[4] C. Bailly, P. Lafon, S. Candel, *Computation of noise generation and propagation for free and confined turbulent flows*, AIAA and CEAS 2nd Aeroacoustics Conference, , No. May.

[5] C. Blom, B. Verhaar, J. van der Heijden, B. Soemarwoto, *A linearized Euler method based prediction of turbulence induced noise using time-averaged flow properties*, 39th Aerospace Sciences Meeting and Exhibit, , No. c.

[6] M. Billson, L.-E. Eriksson, L. Davidson, *Jet Noise Prediction Using Stochastic Turbulence Modeling*, 9th AIAA/CEAS Aeroacoustics Conference and Exhibit, , No. May.

[7] A. Careta, F. Sagués, J. M. Sancho, *Stochastic generation of homogeneous isotropic turbulence with well-defined spectra*, Physical Review E, Vol. 48, No. 3, (1993), pp. 2279–2287.

[8] M. Klein, A. Sadiki, J. Janicka, *A digital filter based generation of inflow data for spatially developing direct numerical or large eddy simulations*, Journal of Computational Physics, Vol. 186, No. 2, (2003), pp. 652–665.

[9] R. Ewert, *Broadband slat noise prediction based on CAA and stochastic sound sources from a fast random particle-mesh (RPM) method*, Computers and Fluids, Vol. 37, No. 4, (2008), pp. 369–387.

[10] M. Dieste, G. Gabard, *Random particle methods applied to broadband fan interaction noise*, Journal of Computational Physics, Vol. 231, No. 24, (2012), pp. 8133–8151.

[11] B. Vanelderen, W. De Roeck, W. Desmet, *Flow noise prediction of confined flows using synthetic turbulence and linearized Euler equations in a hybrid methodology*, 19th AIAA/CEAS Aeroacoustics Conference, (2013), pp. 252.

[12] M. Dieste, *Random-vortex-particle methods applied to broadband fan interaction noise*, Ph.D. thesis, University of Southampton (2011).

[13] R. Kraichnan, *Diffusion by a Random Velocity Field*, Physics of Fluids, Vol. 13, No. 1, (1970), pp. 22.

[14] *Flemish supercomputer centre website*, https://www.vscentrum.be/infrastructure/hardware/hardware-kul, accessed: 2016-05-20.